Chemistry & Biology
Article

Novel Fluorescent Glycan Microarray Strategy Reveals Ligands for Galectins

Xuezheng Song,[1] Baoyun Xia,[1] Sean R. Stowell,[1] Yi Lasanajak,[1] David F. Smith,[1] and Richard D. Cummings[1,*]
[1]Department of Biochemistry, Emory University School of Medicine, Atlanta, GA 30322, USA
*Correspondence: rdcummi@emory.edu
DOI 10.1016/j.chembiol.2008.11.004

SUMMARY

Galectin-1 (Gal-1) and galectin-3 (Gal-3) are widely expressed galectins with immunoregulatory functions in animals. To explore their glycan specificity, we developed microarrays of naturally occurring glycans using a bifunctional fluorescent linker, 2-amino-N-(2-aminoethyl)-benzamide (AEAB), directly conjugated through its arylamine group by reductive amination to free glycans to form glycan-AEABs (GAEABs). Glycans from natural sources were used to prepare over 200 GAEABs, which were purified by multidimensional high-pressure liquid chromatography and covalently immobilized onto N-hydroxysuccinimide-activated glass slides via their free alkylamine. Fluorescence-based screening demonstrated that Gal-1 recognizes a wide variety of complex N-glycans, whereas Gal-3 primarily recognizes poly-N-acetyllactosamine-containing glycans independent of N-glycan presentation. GAEABs provide a general solution to glycan microarray preparation from natural sources for defining the specificity of glycan-binding proteins.

INTRODUCTION

Immunological homeostasis relies on effective expansion of innate and adaptive immune leukocytes during inflammation and contraction of activated leukocytes during resolution of these inflammatory events (Nussler et al., 1999). Failure to appropriately control activated leukocytes following the response often results in damage of viable tissue and can result in autoimmunity. Many factors regulate leukocyte turnover, including members of the tumor necrosis factor (TNF) and galectin families (Elola et al., 2007; Opferman, 2008). TNF family members induce leukocyte contraction through apoptosis, whereas galectin family members induce leukocyte turnover and regulate leukocyte behavior through both apoptotic and apoptosis-independent pathways, depending on the cell type and activation state (Rabinovich et al., 2007a; Stowell et al., 2008b; Toscano et al., 2007b).

In contrast to TNF family members, which engage trimeric counter-receptors through protein-protein interactions, galectins signal through multivalent recognition of cell surface carbohydrate structures (Brewer, 2001; Rabinovich et al., 2007b). However, the carbohydrate structures through which galectins regulate leukocyte viability remain uncertain. Recent studies, using a combined approach of cell surface binding studies and available glycan microarrays, provided key insight into carbohydrate recognition by galectin-1 (Gal-1) and galectin-3 (Gal-3), the two most well-studied galectins. Gal-1 and Gal-3 appear to recognize poly-N-acetyllactosamine ($-3Gal\beta1\text{-}4GlcNAc\beta1\text{-})_n$ (polyLacNAc) cell surface glycans, although the underlying mechanism for this preference appears to fundamentally differ (Leppanen et al., 2005; Stowell et al., 2008a). Other studies suggest that Gal-1 and Gal-3 prefer highly branched complex N-glycans (Guo et al., 2008; Hirabayashi et al., 2002; Walzel et al., 2006) and that galectin signaling is related to N-glycan branching (Lau et al., 2007; Karmakar et al., 2008), but there is uncertainty about the structures and roles of N-glycans in galectin signaling (Carlow et al., 2003; Karmakar et al., 2008). Distinct LacNAc modifications appear to differentially alter Gal-1 and Gal-3 binding to chemically defined and cell surface glycans (Carlow et al., 2003; Leffler and Barondes, 1986; Stowell et al., 2008a).

Although these studies provide insight into the glycan recognition patterns of Gal-1 and Gal-3, the preference of Gal-1 and Gal-3 for LacNAc modifications in the context of N-glycans, as occurs on cell surface glycans, remains uncertain. These uncertainties are due largely to the difficulty in chemically synthesizing complex N-glycans for inclusion on defined glycan microarrays. Although current glycan microarrays contain unprecedented numbers of chemically defined and structurally diverse glycans, many structures represent only terminal glycan structures independent of the context of their expression on glycoproteins as N- or O-linked glycans or on glycolipids (Blixt et al., 2004). Although some glycan binding proteins might only recognize terminal modifications irrespective of the core glycan structure, several studies suggest that the core structure significantly influences terminal glycan recognition (Chandrasekaran et al., 2008; Chiu et al., 1994; Roseman and Baenziger, 2001).

A solution to the problem of presenting naturally occurring, complex glycan structures to potential glycan-binding proteins is to produce a ''natural glycan microarray,'' in which glycans from natural sources are derivatized, separated, and immobilized. This approach is more relevant to biological systems, because glycans can be directly prepared from target cells or tissues. However, for natural glycan microarrays to be practical, strategies for simple and efficient separation and quantification of glycans obtained from natural sources will be required.

Here we report the synthesis of a novel fluorescent linker, 2-amino-N-(2-amino-ethyl)-benzamide (AEAB) and its conjugation to free reducing glycans obtained from natural sources. The resulting glycan-AEAB conjugates (GAEABs) retain fluorescence similar to the glycan-2,6-diaminopyridine (DAP) conjugates reported previously (Xia et al., 2005); however, the arylamine is replaced with a primary alkylamine functional group for more efficient

immobilization onto solid N-hydroxysuccinimide (NHS)-derivatized surfaces. Using this approach, we constructed a glycan microarray incorporating more than 200 glycans from commercially available glycans and glycans obtained from natural sources. With this structurally diverse natural glycan microarray, we evaluated glycan recognition by Gal-1 and Gal-3 and found substantial differences in the types of glycans these galectins recognize. Our studies demonstrate the utility of this novel approach to microarray development and provide a new method for the evaluation of many other glycan binding proteins.

RESULTS

Synthesis of AEAB and Its Conjugation with Glycan

AEAB is synthesized by aminolysis of methyl anthranilate (MA) with ethylenediamine (EDA) (Figure 1a). Because the resulting AEAB possesses both an aromatic and an aliphatic amine, which readily react with hemiacetals of reducing glycans by reductive amination, two conjugates, glycan-AEAB1 and glycan-AEAB2, could theoretically be obtained (Figure 1B). To characterize the products of this reaction, we conjugated the pentasaccharide, lacto-N-fucopentaose III (LNFPIII) (structure 37 in Table S1 available online), with MA by reductive amination followed by aminolysis by EDA to generate only the LNFPIII-AEAB2 conjugate (Figure 1C), which was subjected to high-pressure liquid chromatography (HPLC) analysis (Figure 1D, top). Using well-known reductive amination conditions, free reducing LNPFIII (1–10 nmol) was mixed with 0.35 M AEAB (5 μl) plus 1 M sodium cyanoborohydride ($NaCNBH_3$, 5 μl) in dimethylsulfoxide (DMSO)/acetic acid (AcOH) (7/3 v/v) and heated at 65°C for 2h. As predicted, the conjugation of LNFPIII with AEAB generated two conjugates, presumably LNFPIII-AEAB1 and LNFPIII-AEAB2 (Figure 1D, bottom). By comparing the HPLC profiles (Figure 1D) of the products from the direct conjugation of LNFPIII with AEAB and the EDA aminolysis product of LNFPIII-MA conjugate, LNFPIII-AEAB1 and LNFPIII-AEAB2 were easily identified (Figure 1D). HPLC-purified LNFPIII-AEAB1 and LNFPIII-AEAB2 showed the same mass ([M+Na]+ 1039.326) by matrix-assisted laser desorption/ionization time-of-flight mass spectrometry (MALDI-TOF MS) analysis (Figure 1E), which matched the calculated theoretical value ([M+Na]+ 1039.407).

Optimization of Glycan-AEAB Conjugation

Glycan-AEAB2 conjugates are desirable because they have a primary alkylamine group, which is more reactive than arylamine groups. To improve the chemoselectivity between the arylamine and alkylamine groups on AEAB, we varied the acidity of the reaction using the model compound LNFPIII. The ratio of LNFPIII-AEAB1 to LNFPIII-AEAB2 was analyzed by HPLC on a porous graphitized carbon (PGC) column (Figure 2a) as a function of varying amounts of AcOH in the reaction mixture. When pure DMSO was used as the solvent for derivatization, the reaction was very slow and impractical. As the amount of AcOH was increased from 10% to 40%, the preferred product shifted from LNFPIII-AEAB1 to LNFPIII-AEAB2 (Figure 2A). This indicated that at higher acidity, reductive amination via the arylamine was favored over the alkylamine, consistent with the aliphatic amine being more nucleophilic and basic than the aromatic amine and therefore more likely to be protonated (Figure 2B). After protonation, the nucleophilicity of the aliphatic amine dramatically decreases so that the unprotonated aromatic amine became more reactive toward the reducing end of glycans to form a Schiff's base, which was reduced by $NaCNBH_3$ to give the final glycan-AEAB2 conjugate.

To further increase the protonation of AEAB and make a more convenient reagent, we treated AEAB with excess hydrochloric acid before its conjugation with glycans. The conjugation of LNFPIII with this pre-protonated AEAB hydrochloride salt in DMSO/AcOH (7/3 v/v) gave LNFPIII-AEAB2 as the dominant product with only trace amounts of LNFPIII-AEAB1 (Figure 2A). When an aliphatic amine is totally protonated, it loses its reactivity toward aldehydes. The reductive amination of an aromatic amine with reducing glycans, however, is not dramatically affected by protonation due to its lower basicity. One concern with the AEAB-HCl salt is that its acidity might affect sialic acid residues on glycans. We evaluated this by comparing HPLC profiles of LS tetrasaccharide c (LSTc)-2-aminobenzoic acid (2AB) conjugate versus the LSTc-AEAB conjugate (Figure 2C) and by testing the profiles of sialyllactose versus lactose by HPLC (Figure 2D). It is known that 2AB conjugation under this condition does not affect sialic acid residues (Bigge et al., 1995). The similarities of the HPLC profiles of LSTc-2AB and LSTc-AEAB, and the lack of a peak corresponding to lactose in the sialyllactose samples indicated no significant desialylation ($\leq$1%) during AEAB conjugation under the above reductive amination conditions.

To address the conjugation efficiency of AEAB with reducing glycans, we compared the profiles of free reducing LNFPIII and the crude AEAB conjugation product by high-pH anion-exchange chromatography with pulsed amperometric detection (HPAEC-PAD) (Figure 2E). The results show that more than 98% of the reducing LNFPIII was converted to LNFPIII-AEAB under the above reaction conditions. The conjugation efficiency of AEAB with glycans was not dependent on the glycan structure.

Printing Efficiency of Different Glycan Conjugates on Surface-Activated Glass Slides

To explore the use of AEAB for constructing glycan arrays, the printing efficiency of LNFPIII-AEAB1 and LNFPIII-AEAB2 were tested on NHS- and epoxy-activated glass slides. LNFPIII-AEAB1, LNFPIII-AEAB2, and LNFPIII-DAP were printed side by side along with free LNFPIII, DAP, and AEAB as controls. The printing (coupling) efficiency was indirectly estimated by fluorescent lectin binding. Biotinylated *Aleuria aurantia* lectin (AAL) detected with cyanine 5-streptavidin (Cy5-SA) was used to detect immobilized LNFPIII. On NHS slides (Figure S1A), the stronger fluorescence signal of LNFPIII-AEAB2 compared with LNFPIII-AEAB1 supports the conclusion that LNFPIII-AEAB2 possesses the more reactive primary alkylamine group (Figure 1b). LNFPIII-AEAB2 can be detected at ~2-fold lower printing concentration than LNFPIII-DAP and ~4-fold lower printing concentration than LNFPIII-AEAB1, indicating an enhanced printing efficiency. On epoxy slides, the minimum detectable printing concentrations are lower than on NHS slides. Thus, whereas epoxy slides provide somewhat higher sensitivity, the reaction is less specific (Figure S1B); that is, underivatized LNFPIII, free AEAB, and DAP show undesirable, nonspecific binding signals. Unexpectedly, on epoxy slides, LNFPIII-AEAB2 does not show a lower

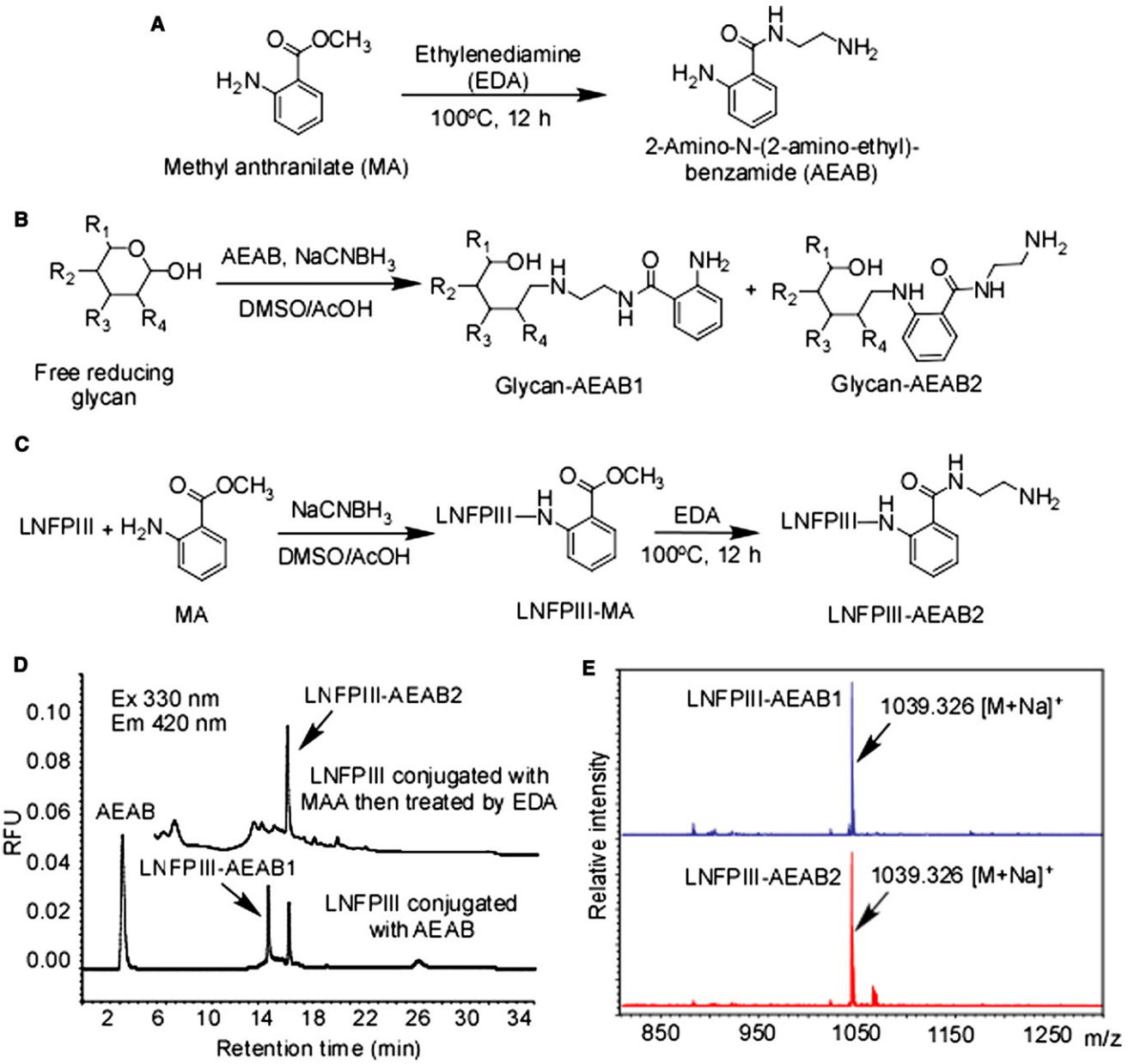

Figure 1. The Synthesis of AEAB and Its Conjugation with Glycans

(A) Synthesis of AEAB.

(B) Expected products of conjugation of AEAB with glycans.

(C) Conjugation of LNFPIII with MA, treated with EDA to give only LNFPIII-AEAB2.

(D) HPLC profiles of EDA treatment of LNFPIII-MA conjugate (top) and the direct conjugation of LNFPIII with AEAB under normal reductive amination condition (bottom).

(E) MALDI-TOF MS spectra of HPLC-purified LNFPIII-AEAB1 and LNFPIII-AEAB2.

minimum detectable concentration than LNFPIII-AEAB1, although both show lower minimum detectable concentrations than LNFPIII-DAP. It is possible that dual reactions on epoxy through both the primary arylamine and secondary alkylamine functional groups of LNFPIII-AEAB1 might occur, because they are similarly reactive toward epoxy. Therefore, its printing efficiency is even higher than that of LNFPIII-AEAB2, which bears a highly reactive primary alkylamine and an inert secondary arylamine. Nevertheless, the strong signals from LNFPIII-AEAB2 on both NHS and epoxy slides show the utility of AEAB as a fluorescent linker for natural glycan array development. Similar to LNFPIII-DAP, immobilized LNFPIII-AEAB2 showed weak direct fluorescence signals when the array was scanned using excitation 495 nm and emission 520 nm (data not shown), although these wavelengths are far from the optimal excitation 330 nm and emission 420 nm. Although weaker than that of LNFPIII-DAP, the

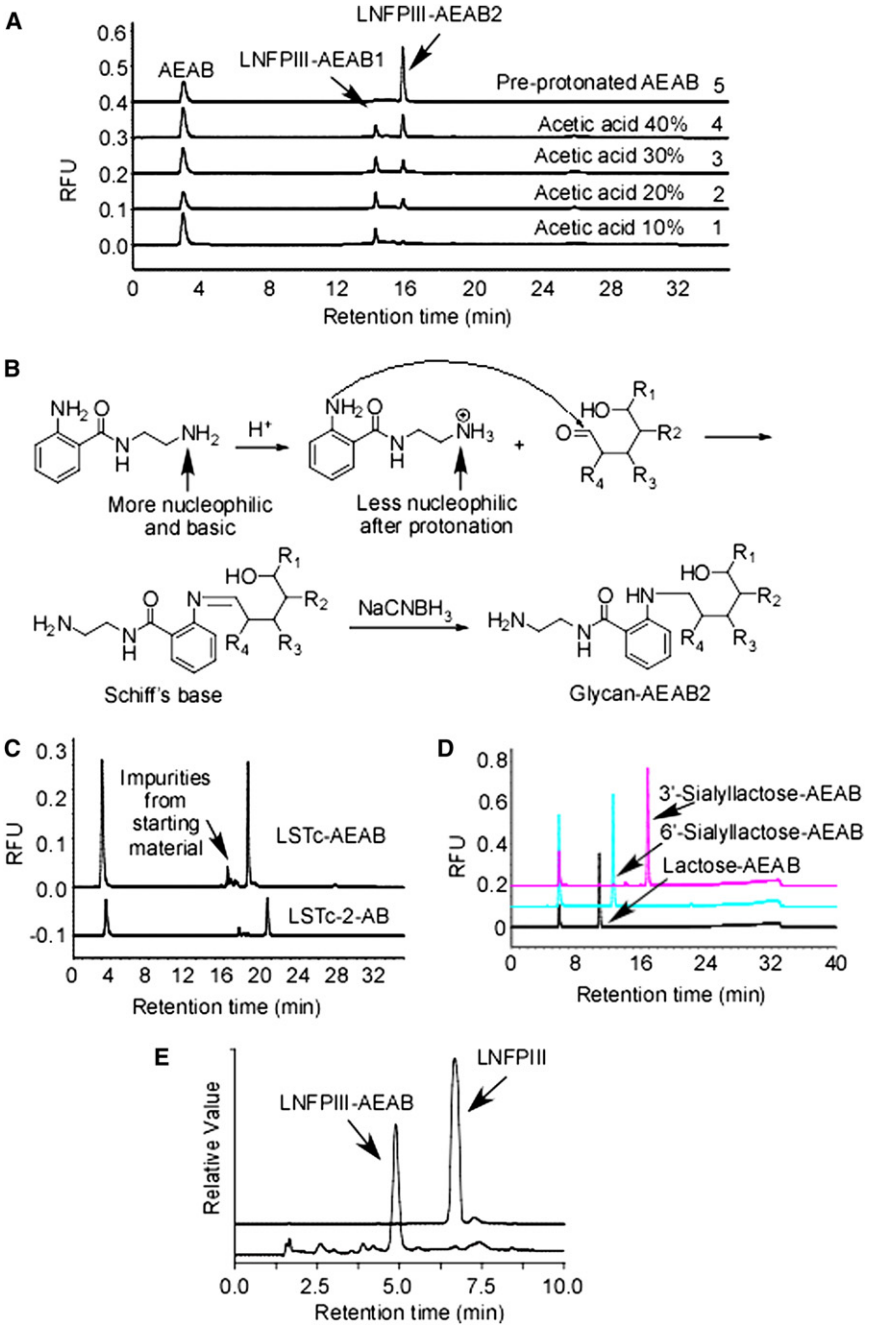

Figure 2. The Optimization of AEAB Conjugation Using LNFPIII

(A) HPLC profiles of AEAB conjugated with LNFPIII at different conditions of acetic acid and with the pre-protonated HCl salt of AEAB.

(B) Proposed mechanism of the acidity effect on the chemoselectivity between arylamine and alkylamine during the AEAB derivatization.

(C) Comparison of HPLC profiles of LSTc-2AB and LSTc-AEAB.

(D) Comparison of HPLC profiles of 3′-sialyllactose, 6′-sialyllactose, and lactose.

(E) HPAEC-PAD profiles of free reducing LNFPIII and crude AEAB conjugation product.

off-peak fluorescence of AEAB is sufficient for grid localization and quality control of the glycan microarray while not interfering with subsequent binding assays (Song et al., 2007; Xia et al., 2005). With the future development of ultraviolet irradiation (UV) lasers for microarray scanners, accurate on-slide quantification can be expected with the AEAB linker.

We have shown previously that fluorescent glycan conjugates prepared with arylamines using DAP can be used to construct quantifiable glycan microarrays on epoxy slides (Song et al., 2007). Recently it was reported that 2AB and 2AA glycan derivatives can be used for printing natural glycan microarrays on epoxy-derivatized slides (de Boer et al., 2007). The covalent linkage of the glycan derivatives to epoxy is through the secondary arylamine, formed when 2AA or 2AB are coupled to reducing glycans via reductive amination. Although reactivity of this secondary amine to epoxy slides is sufficient for preparing microarrays of derivatized glycans, this functional group is not bound by NHS-derivatized slides. More importantly, as shown in Figure S1C, AEAB conjugates couple with much higher efficiency than those of 2AA and 2AB when printed on either NHS or epoxy slides. Based on the high efficiency of printing, the low background binding, and the flexibility of AEAB derivatives on different activated surfaces, we used glycan-AEAB conjugates for preparing natural glycan arrays.

Construction of a 52-GAEAB Microarray from Free Reducing Glycans

To demonstrate the utility of the AEAB linker, we prepared GAEABs from 52 commercially available, free reducing glycans, which are shown as symbols in Table S1. The GAEAB derivatives from 1 to 10 nmol of each pure glycan were purified using HPLC by following their fluorescence and UV absorption. Each GAEAB was quantified and adjusted to a final concentration of 100μM for printing. Together with four controls (AEAB, underivatized LNFPIII, buffer, and biotin-hydrazine), the 52 GAEABs were printed in replicates of 6 on NHS-activated slides. A total of 14 replicated subarrays containing 56 samples were printed on each slide. The printing format for constructing this GAEAB microarray is shown in Figure S2. Some duplicate structures do occur on the array, decreasing the total number of unique glycans, but the duplicate structures serve as an internal control.

After printing, slides were incubated and blocked as described in Experimental Procedures. A single rehydrated slide was fitted with a silicon grid separating the slide into 14 chambers, isolating

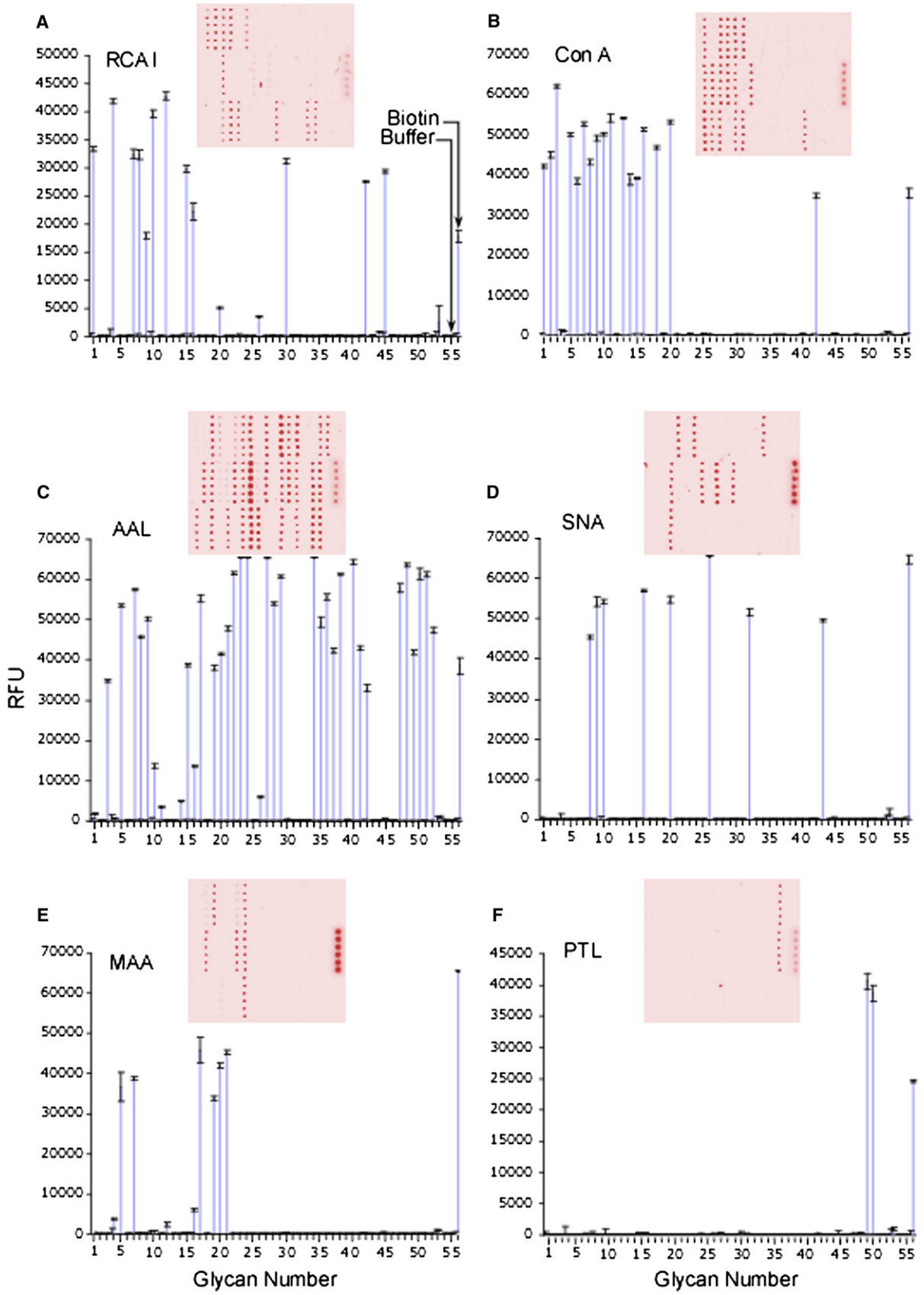
A
RCA I
Biotin
Buffer
B
Con A
C
AAL
D
SNA
E
MAA
F
PTL
RFU
Glycan Number
Glycan Number

each subarray. Each subarray can be interrogated individually with various biotinylated lectins that are subsequently detected by Cy5-SA. For each lectin analyzed, a histogram representing average relative fluorescence units (RFU) bound to each glycan is shown in Figure 3. The fluorescent image for the corresponding lectin is shown as an insert in its histogram. All histograms in Figure 3 showed expected binding specificity with an excellent signal/noise ratio and high precision of measurement (%CV < 10%). For example, *Ricinus communis* agglutinin I (RCA-I) bound well to glycans having terminal nonreducing β1,4-linked Gal residues, known to be high-affinity ligands for RCA-I (Cummings, 1994; Merkle and Cummings, 1987; Yamamoto et al., 1998). However, it does not bind to lactose-AEAB, possibly because of the open-ring structure of the neighboring glucose unit. Each of the other lectins showed similar predicted specificity, such as concanavalin A (Con A) recognition of mannose-containing glycans, AAL binding to fucosylated glycans, *Sambucus nigra* agglutinin (SNA) and *Maackia amurensis* agglutinin (MAA) binding to sialylated glycans, and *Psophocarpus tetragonolobus* lectin (PTL) binding to blood group A (Pueppke, 1979). These results demonstrate the robust utility of the preparation and printing of GAEABs prepared from large, complex glycans that would be impractical to synthesize chemically. The validity of the array is confirmed by the specificity of the lectins detecting GAEABs printed on the NHS-derivatized slides. Although most lectin binding was specific for the expected glycan, AAL, for example, bound several nonfucosylated glycans. This binding is likely due to the high concentration of lectin used, which can highlight binding to weakly recognized glycans on the microarray. In the subarray analyses, AEAB linker alone (#53), buffer (#55), and the underivatized LNFPIII (#54) showed no binding, whereas the biotin-hydrazide (#56), was detected on all subarrays by Cy5-SA (Figure 3).

N-Glycan Release, Conjugation, and 2D-HPLC Separation

Several commercially available glycoproteins, including chicken ovalbumin, bovine fetuin, bovine immunoglobin G (IgG), and porcine thyroglobulin, were selected for expansion of the natural glycan microarray. The overall workflow for generating "natural glycans" from natural products is shown in Figure 4. N-glycans were released from denatured glycoproteins as described in Experimental Procedures. The free reducing N-glycans were conjugated with AEAB, and the fluorescent-labeled glycan mixture was separated by 2-dimensional (2D) HPLC. GAEABs were readily separated using a combination of chromatographic methods including an amide or normal phase (NP) column, a C18 reverse phase (RP) column, or a PGC column. These orthogonal methods are useful for multi-dimensional-HPLC purification of GAEABs. For all three columns, acetonitrile and water were used as the solvents. With the NP column, ammonium acetate salt was used as the modifier whereas 0.1% TFA was used as the modifier for both RP and PGC columns. The NP or RP column was chosen for the first-dimension HPLC separation, and the PGC column was always chosen for the second-dimension separation because of its excellent resolution and desalting effect. A typical 2D-HPLC separation for N-glycans released from ovalbumin is shown in Figure 5. In Figure 5A, 20 fractions from NP HPLC were collected, and each fraction was further fractionated by the PGC column (Figure 5B). Fractions appearing to contain near-homogeneous GAEABs were collected, and the collected samples were dried, reconstituted, and repurified using a short PGC cartridge, which allowed for purification to homogeneity and quantification. Each fraction containing a defined amount of GAEAB derivative was dried and dissolved in printing buffer to a final concentration of 100 μM. These solutions were used to print each glycan in triplicate on the NHS-activated glass slides, generating a natural N-glycan microarray. Glycan released from other glycoproteins, such as bovine fetuin, IgG, and thyroglobulin, were derivatized and processed for printing using the same method. By incorporating all fractions and 84 GAEABs individually prepared from commercially available oligosaccharides and defined free glycans, we constructed a glycan microarray with more than 200 glycans within each of 14 subarrays on a single slide. Table S2 provides a description of the glycans printed on this array. We have noted the presence of N-glycans with only 1 GlcNAc instead of ≥2, presumably due to the known contamination of some commercial PNGaseF with endo-beta-N-acetylglucosaminidase F activity. The defined glycans are shown in symbols and the natural glycans are represented by their compositional analysis determined by MALDI-TOF MS.

Nomenclature and Compiling of GAEAB Fractions

Due to the rapid production of large numbers of GAEABs using this natural glycan array technology and the fact that detailed sequence analysis is not necessary if the glycan is not detected by a glycan binding protein, we simply identified the fractions systematically for easy data collection and analysis. Naming isolated GAEAB fractions was based on the HPLC separation procedure. For example, bovine IgG-AEAB-NP03-PGC02 represents four columns of information, which designate the source (bovine IgG), derivatization method (AEAB), first dimension of NP HPLC fraction number (NP03), and second dimension of PGC HPLC fraction number (PGC02), respectively. More columns of information can be added, such as additional separation steps and the

Figure 3. Lectin-Binding Assay on a 52 GAEAB Microarray

Subarrays were separated by incubation chambers and incubated with various biotinylated lectins followed by Cy5-SA. The Cy5 fluorescence image is scanned and shown as the red, 10 mm × 10 mm insert. The error bars represent the standard deviation of six replicates.

(A) RCA I binds to terminal Galβ1,4-GlcNAc.

(B) Con A binds to all N-glycans but not triantennary and tetra-antennary complex type N-glycans.

(C) AAL binds to all fucose-containing glycans.

(D) SNA binds to terminal α2,6-sialic acid.

(E) MAA binds to Neu5Acα2-3Galβ1,4-.

(F) PTL binds to blood group A tetrasaccharide and pentasaccharide. Biotin spots printed on each subarray serve as an alignment feature to localize each subarray on the slide.

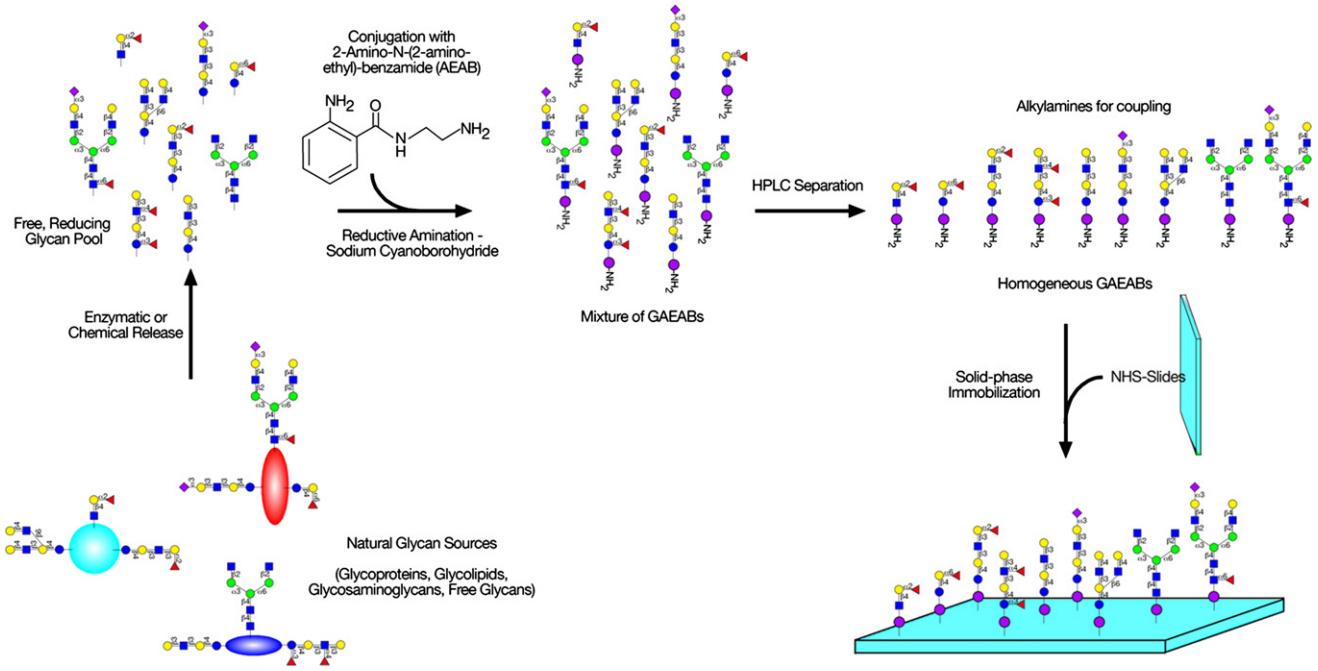

Figure 4. The General Strategy of Natural Glycan Array Development Using Complex Glycoconjugates as Starting Materials

mass of the glycan. Thus, a glycan mapping system can be devised based on HPLC retention time and MS data as a large library is constructed. A clear, easily expandable, and searchable database for the GAEAB fractions is essential for computer-assisted high-throughput analysis, especially because the potentially unlimited GAEAB library will rapidly expand.

MALDI-TOF MS of GAEAB Fractions

All GAEAB fractions were characterized by MS. Figure S3 shows examples of the MS and MS/MS spectra of two fractions from bovine IgG, neutral bovine IgG-AEAB-NP05-PGC01, and sialylated bovine IgG-AEAB-NP14-PGC02. All neutral GAEABs gave clean MS spectra and informative MS/MS data. Composition and tentative structures of neutral glycans can be assigned according to the MS data and published information on glycans from various sources. The fragmentation pattern in Figure S3A shows losses of a deoxyhexose (−146) and a HexNAc (−203), respectively, suggesting a fucosylated biantennary structure with one branch degalactosylated. Figure S3B shows the MS and MS/MS spectra of a monosialylated glycan. It is clear that in positive mode, desialylation fragmentation is observed. The fragmentation pattern of the desialylated parent ion at 1810.6 is almost identical to that of Figure S3A, indicating the same skeletal structure. In negative mode analyses, however, a single peak is observed, confirming the existence of a terminal Neu5Gc (±307). Combining the information from MS and MS/MS spectra in different modes, the composition and structure of acidic sugars can also be proposed.

Binding of Gal-1 and Gal-3 on the Natural Glycan Microarray

The availability of this large glycan array (>200 glycans) composed of many high-molecular-weight, complex, multiantennary N-glycans allowed us to explore the glycan binding specificity of human Gal-1 and Gal-3 (Camby et al., 2006; Dumic et al., 2006; Ohtsubo et al., 2005; Stowell et al., 2007) in greater depth. These galectins are thought to recognize polyLacNAc sequences in N- and/or O-glycans (Leppanen et al., 2005; Stowell et al., 2008a), but existing microarrays have few large, complex N-glycans to allow testing of the galectin binding specificity (http://www.functionalglycomics.org/).

Gal-1 and Gal-3 exhibited somewhat similar binding patterns when evaluated at relatively high concentrations (6–7 μM) (Figures 6A and 6B). At these concentrations their glycan specificity was similar to that reported with Gal-1 exhibiting higher binding toward N-glycans and Gal-3 recognizing blood group antigens, thus generally validating this overall natural glycan microarray relative to available microarrays (Stowell et al., 2008a). Furthermore, α2-6 sialylation blocked Gal-1 and Gal-3 recognition, whereas α2-3 sialylation had no effect on binding, consistent with prior findings (Stowell et al., 2008a). However, because many ligands were bound at near-saturating levels (40,000–50,000 RFU) using this high concentration of galectins, we evaluated the binding at lower concentrations (1.5 μM and lower, Figures 6C–6F), which reflect physiological lectin levels. We found previously that both Gal-1 and Gal-3 recognize cell surface glycans at submicromolar levels (Leppanen et al., 2005; Stowell et al., 2008a). At less than 1 μM, Gal-1 and Gal-3 exhibited striking differences in their glycan recognition. Gal-1 displayed significant binding toward many N-glycans, including glycans 001, 011, 025, and 094 (Figure 6E and Table S3). All of these glycans are characterized by biantennary presentation of terminal β4-linked galactose. By contrast, Gal-3 at this concentration did not bind those N-glycans, but rather recognized glycans containing a repeating unit of Gal-GlcNAc (LacNAc), as found in glycans 016, 026, and 078 (Figure 6F and Table

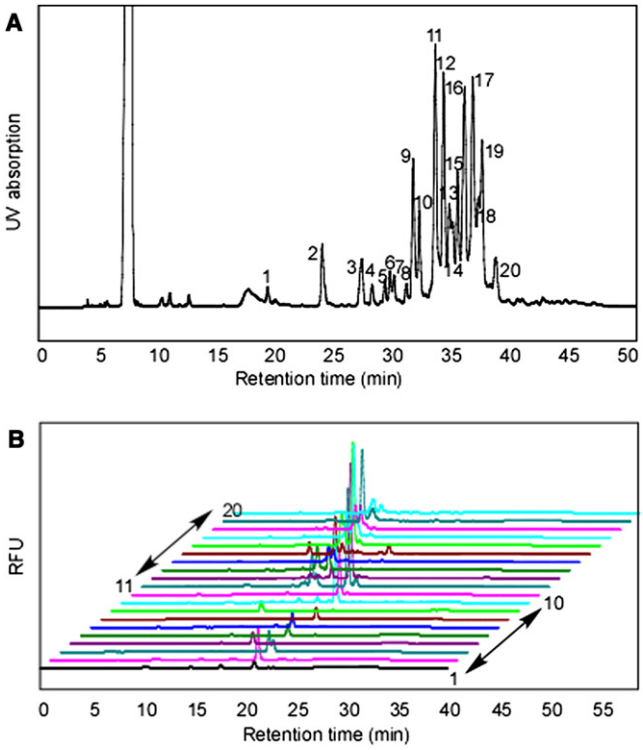

Figure 5. 2D-HPLC Separation of Fluorescent-Labeled Glycans Released from Ovalbumin

(A) First-dimension HPLC separation using NP column.

(B) Second-dimension HPLC separation of glycans collected from (A) using PGC column.

S3). The extended glycans 026 and 078 contain Galβ1-3 linkages, rather than Galβ1-4 linkages, as found in glycan 016. The ability of Gal-3 to bind glycans such as 026 and 078 is novel to our study, because such glycans are not presently available on the glycan microarray from the Consortium for Functional Glycomics (CFG). Previous studies have showed that short (Galβ1-3GlcNAc or Galβ1-3GlcNAcβ1-3Galβ1-3GlcNAc) type 1 glycans are not bound by Gal-3 (Stowell et al., 2008a). These results demonstrate that although Gal-1 and Gal-3 exhibit high affinity for some N-glycans, each possesses distinct differences in N-glycan recognition, providing the first significant differences in the recognition of naturally occurring glycans by these two lectins. Gal-3 significantly preferred glycans containing LacNAc repeating units, as found in polyLacNAc cell surface glycans.

DISCUSSION

The strategy we have employed for natural glycan microarray development is shown in Figure 4. A complex mixture of glycans derived from naturally occurring glycoconjugates by chemical or enzymatic procedures is derivatized with a bifunctional fluorescent linker AEAB using a quantitative and glycan-specific method. The fluorescent glycan mixture is separated into individual components by chromatographic methods and individually characterized by MS and other methods to define their structures. The purified glycans are immobilized onto a solid phase through their primary alkylamine, directly or after being activated to another suitable functional group.

Glycan microarrays have been produced from naturally occurring glycans using nonfluorescent linkers for coupling glycans to solid surfaces (Feizi and Chai, 2004; Feizi et al., 2003). Fluorescent linkers provide two important advantages for developing microarrays. First, the fluorescent tags produced by glycan-specific reductive amination incorporates 1 mol label per mol glycan to provide a detection method for monitoring the purification and for quantifying individual glycans, which are otherwise not detected by simple, nondestructive spectrophotometric methods. Second, the fluorescent tag permits the application of this approach to glycans derived from cell and tissue glycoconjugates, which are generally available in only limited quantities. For example, preparation of glycan microarrays using fluorescent-tagged glycans requires only 1 to 2 nmol of each fluorescent glycan (10–20 μl of a 100 μM solution); because noncontact printing can deliver 333 pl at 5% intertip variation, this amount of material could print thousands of microarrays with each glycan printed in triplicate.

We have shown that free reducing glycans can be readily derivatized with the novel fluorescent linker AEAB to generate GAEAB derivatives that are efficiently derivatized to either NHS- or epoxy-activated glass slides. Although both amino groups of AEAB can potentially react with the reducing glycan by reductive amination to give two isomers, we successfully differentiated the two amino groups by using the AEAB-HCl salt for glycan derivatization. The simple AEAB derivatization is a mild reaction analogous to other commonly used fluorescent labels (2AB and DAP). GAEAB derivatives, shown here to be superior to previously described fluorescent linkers, provide a new direction for generating large libraries of naturally occurring glycans from cell and tissue glycoconjugates because this derivatization does not affect relatively labile sialic acid and sulfate residues on glycans. The derivatives have excellent separation characteristics on HPLC as shown in Figure 5; unlike many fluorescent derivatives, they are amenable to MS analysis directly by MALDI/TOF or by spectrometric analysis of permethylated derivatives (data not shown), and coupling via the alkylamine to NHS-derivatized glass slides is quite efficient in preparing microarrays.

Our previous study showed that DAP derivatization of glycans (Song et al., 2007; Xia et al., 2005) is an appropriate method for natural glycan array development, especially on epoxy-activated slides. However, the relatively low reactivity of the arylamine derivative of the glycans toward various leaving groups compared with the aliphatic amine derivative AEAB limited this approach to epoxy-derivatized slides, where the highly reactive epoxy groups react with both primary and secondary amines, and in some cases might react with hydroxyl groups, causing a heterogeneous presentation of glycans on an array. Epoxy-derivatized slides also generated much higher backgrounds with complex samples due to nonspecific binding of fluorescent detecting reagents, thus making them less desirable when highly sensitive detection is required. For these reasons, common fluorescent derivatives such as 2AA and 2AB, which can only be printed on epoxy slides (de Boer et al., 2007), are not as desirable as AEAB and other bifunctional fluorescent linkers having an alkylamine available for coupling to derivatized surfaces.

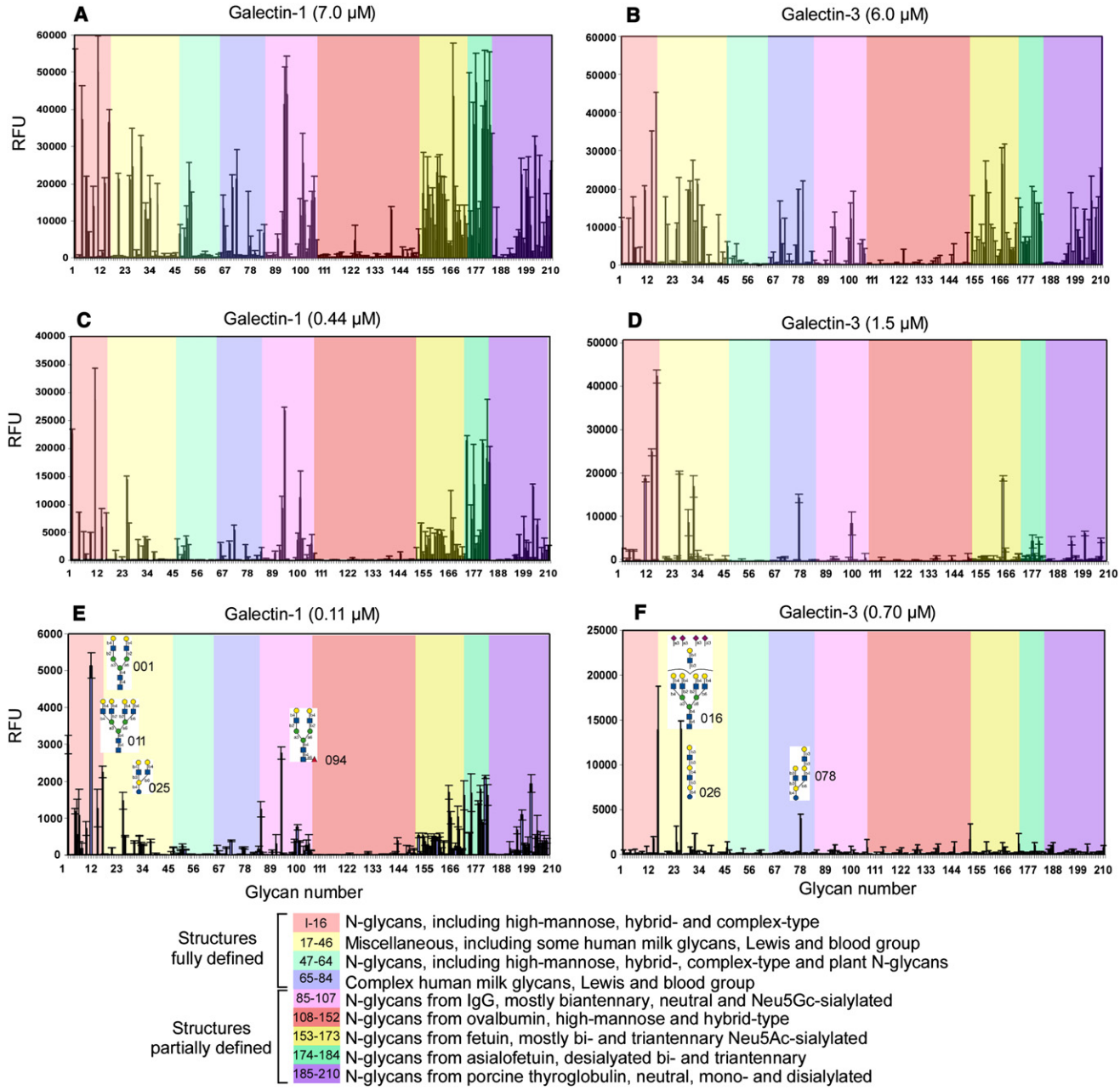

Figure 6. The Binding of Gal-1 and Gal-3 on the GAEAB Glycan Array

(A) Gal-1 at 7 μM. The natural sources of the GAEABs are marked with different colors. Glycan 016 is a mixture of isomers with an 80/20 ratio. The error bars represent the standard deviation of three replicates.

(B) Gal-3 at 6 μM.

(C) Gal-1 at 0.44 μM.

(D) Gal-3 at 1.5 μM.

(E) Gal-1 at 0.11 μM.

(F) Gal-3 at 0.7 μM.

Using this novel fluorescent derivatization method, we derivatized many commercially available, free reducing glycans (Table S1) using only 1–10 nmol (1–50 μg) of glycan. Thus, natural glycan sources can be employed as an almost unlimited library of glycan structures. By contrast, most glycans included in printed glycan microarrays, such as those of the CFG, are chemically or enzymatically synthesized (Blixt et al., 2004), and typically milligrams of each glycan are required for maintaining a nonfluorescent glycan library. For this reason, nontagged glycan libraries and their corresponding microarrays will expand slowly, because of the high cost and difficulty of chemical synthesis. With the technique described here, more than 200

GAEABs were generated from free glycans released from commercially available glycoproteins in a rapid and parallel fashion. More importantly, the GAEAB library can be easily expanded, using unlimited glycan sources from nature. In this GAEAB library, 35 GAEABs were prepared from complex N-glycan structures that are not available on the CFG glycan array, because of their difficult synthesis. Many sialylated and sulfated glycans were also included to represent the structural diversity, which proved the general applicability of this fluorescent derivatization method on different glycan structures. Recently, an N,O-dialkylamine was developed as a new bifunctional linker for glycan derivatization (Bohorov et al., 2006). Although this approach can retain the ring-closed structure of free reducing glycans, the glycan cannot be detected by common sensitive spectrophotometric or fluorometric methods. Therefore, it is useful only for pure compounds that are available in large quantities. The AEAB fluorescent derivatization successfully circumvents these problems without diminishing printing efficiency. Although AEAB derivatives possess a reduced terminal monosaccharide, most carbohydrate recognition by glycan binding proteins involves recognition of the nonreducing end of glycans.

In natural glycan array development, a mixture of many glycans from natural sources can be derivatized and separated. To confirm that the AEAB fluorescent derivatization of glycans is nonselective and nearly quantitative, we compared the fluorescent labeling of glycans with different labels. The high similarity of the HPLC profiles of fetuin-derived glycans conjugated with 2AB, DAP, and AEAB demonstrated that derivatization by AEAB is nonselective toward different glycans. Using appropriate solvent systems, the GAEAB mixtures can be separated using various HPLC columns, such as amine NP column, C18 RP column, and PGC column. These HPLC columns have very different retention mechanisms, thus providing the orthogonal methods required for multidimensional chromatography. By choosing appropriate HPLC columns, complex glycan mixtures from human milk or mixtures released from glycoproteins, cells, or tissues can be conjugated with AEAB and quickly separated in one or more dimensions. The purified fractions can be quantified, characterized, and printed on surface-activated glass slides. We released, labeled, and separated a large number (>125) of N-glycans using this strategy by starting from several commercially available, naturally occurring glycoproteins. These homogeneous fractions were characterized with MALDI-TOF MS and various lectins. Combined with the GAEABs prepared directly from purified, commercially available glycans, we constructed a glycan microarray incorporating more than 200 glycans, most of which are complex N-glycans not available on the CFG glycan array. Although the fully defined CFG glycan array is most useful for screening glycan-binding proteins for binding motifs to determine specificities and relative affinities of glycans for glycan-binding proteins, natural glycan arrays of cells and tissues composed of partially defined glycans that bind biologically relevant macromolecules will be useful for confirming the definition of a natural ligand and will permit discovery of new protein-carbohydrate interactions. Although many glycans separated by multidimensional HPLC might have similar carbohydrate compositions, their separation indicates that they are structurally different. In addition, it is possible that even a single peak of isolated glycan might have a unique composition, but be composed of structural isomers that copurified. Future studies on such glycans will include additional HPLC-MS/MS mapping systems, 3D-HPLC purification of nonhomogeneous fractions, and more structural characterizations of glycans.

Although previous studies suggest a general preference of galectin family members for polyLacNAc glycans (Leppanen et al., 2005; Stowell et al., 2008a), in the present study Gal-1 and Gal-3 displayed differential binding at submicromolar concentrations of protein toward complex N-glycan and polyLacNAc-containing glycans. Gal-1 exhibited relatively similar affinity toward many different complex N-glycans, especially those expressing ≥ 2 terminal, nonreducing β4-linked galactose residues. The specific binding of galectin-1 to N-glycans is consistent with recent findings (Karmakar et al., 2008) that cell binding and signaling are dependent on the expression of complex-type N-glycans. By contrast, Gal-3 only recognized glycans containing a polyLacNAc extension. This preference provides the first biochemical basis for several studies suggesting that N-glycans and polyLacNAc elongation differentially contribute to galectin signaling, as has been observed in studies on T cell activation and GLUT-2 cell surface half-life through galectin-ligand interactions (Breuilh et al., 2007; Lagana et al., 2006; Lajoie et al., 2007; Ohtsubo et al., 2005; Wilker et al., 2007) and implicate Gal-3, along with Gal-1 and Gal-9, as key regulators in these processes. Furthermore, the differential glycan recognition displayed by Gal-1 and Gal-3 toward distinct N-glycans might underscore the differential sensitivity of T cells and other cell types to Gal-1 and Gal-3 (Camby et al., 2006; Cao et al., 2002; Frigeri et al., 1993; La et al., 2003; Rubinstein et al., 2004; Toscano et al., 2007a). Importantly, there are many N-glycans on human leukocytes, especially neutrophils, that are complex highly branched chains expressing polyLacNAc (Babu et al., 2008). The specific, high-affinity interactions of Gal-1 and Gal-3 for these biologically relevant N-glycans would not have been recognized without the development of the natural glycan array. The dose-dependent method utilized on the array is important when both high- and low-affinity ligands are present, helping to identify the high-affinity ligands, which are defined as those ligands that continue to be bound by lectin at very low lectin concentrations. Additionally, interesting observations were made regarding the fine specificity of galectin binding. Small structural differences in glycans, for example the core fucosylation of glycan 051, dramatically decreased the binding to Gal-1. Future studies using the type of natural glycan microarray described here will permit comparison between galectin family members for specific glycan recognition. In addition, such natural glycan microarrays will be useful for screening many types of glycan binding proteins from other sources, such as viruses, bacteria, and serum proteins.

SIGNIFICANCE

Recognition of complex carbohydrates by glycan binding proteins is the primary manner by which the glycome is interpreted to provide information on biological processes. However, modern glycomic research shows that each cell and tissue of every organism generates a wide variety of glycans and each cell type has a distinctive repertoire of glycan structures. In addition, hundreds of glycan binding proteins have been identified and many more are predicted

to occur. To define the interactions between these large groups of interacting molecules, new chemical approaches are needed. The most successful strategy to date has been glycan microarrays using chemically synthesized glycans. However, chemical synthesis alone only provides libraries of known structures that are amenable to the current synthetic mechanisms. Practical libraries of large, complex glycans and from novel naturally occurring glycans will only be available through the development of glycan microarrays from naturally occurring glycans. Here we have described a fluorescent linker strategy for rapidly, quantitatively, and inexpensively derivatizing glycans to solid surfaces such as glass slides. This new approach permits the preparation of glycan microarrays that are amenable to the use of naturally occurring glycans from biological sources. Molecular recognition of glycans by glycan binding proteins, as found in soluble forms and in cell membranes of all organisms, will be more readily explored using natural glycan microarrays generated by this approach.

EXPERIMENTAL PROCEDURES

Free reducing sugars (stored at −20°C) were purchased from V-labs, Inc. and Glycoseparations (http://www.glycoseparations.com). All chemicals were purchased from Sigma-Aldrich and used without further purification. HPLC solvents were purchased from Fisher Scientific. PNGase F was purchased from New England Biolabs. An Ultraflex-II MALDI-TOF/TOF system from Bruker Daltonics was used for MALDI-TOF MS analysis of glycan conjugates. Plant lectins were purchased from EY Labs and used at 10 μg/ml for each lectin. Printing of glycan arrays was performed using a Piezorray Printer (Perkin Elmer) and analysis of glycan arrays was accomplished by scanning with a ProScanArray Scanner (Perkin Elmer) equipped with 4 lasers.

Synthesis of AEAB

AEAB was synthesized by reacting MA with EDA, as described in the Supplemental Data.

Conjugation of Free Reducing Oligosaccharides with DAP, AEAB, and MA

The fluorescent conjugation of glycans with DAP, AEAB hydrochloride salt, and MA followed an established procedure (Xia et al., 2005) with slight modification (described in Supplemental Data).

Release of Glycans from Glycoproteins by PNGase F Digestion

PNGase F digestion was done according to the manufacturer's instructions. Denaturing buffer, NP40, and G7 buffer were supplied by the manufacturer.

HPLC

HPAEC-PAD analysis was performed with a Dionex ICS-3000 system on a Carbopac PA-100 column. The elution gradient was set to 2.5–125 mM sodium acetate in 100 mM sodium hydroxide over 50 min. HPLC analysis and separation of GAEABs was done on a Shimazu HPLC CBM-20A system coupled to a UV detector SPD-20A and a fluorescence detector RF-10Axl. UV absorption at 330 nm or fluorescence at 330 nm excitation and 420 nm emission was used to detected glycan conjugates with DAP, 2AB, and AEAB in HPLC analysis and separation. Both UV absorption and fluorescence intensity were used for the quantification of GAEABs using LNFPIII-AEAB as a standard. More details are described in Supplemental Data.

Generation of Recombinant Human Gal-1 and Gal-3

Human galectins were prepared as outlined previously (Stowell et al., 2004). The affinity purification and biotinylation are described in Supplemental Data.

Printing, Binding Assay, and Scanning

NHS-activated slides were purchased from Schott. Epoxy slides were purchased from Corning. Noncontact printing was performed using a Piezorray Printer (Perkin Elmer). Biotinylated lectins were used in the binding assay and the bound lectins were detected by a secondary incubation with Cy5-SA. The slides were scanned with a Perkin Elmer ProScanArray microarray scanner equipped with 4 lasers covering an excitation range from 488 to 637 nm. The scanned images were analyzed with the ScanArray Express software. All images obtained from the scanner are in grayscale and colored for easy discrimination.

SUPPLEMENTAL DATA

The Supplemental Data include Supplemental Experimental Procedures, three tables, and three figures and can be found with this article online at http://www.cell.com/chemistry-biology/supplemental/S1074-5521(08)00450-X.

ACKNOWLEDGMENTS

This work was supported by in part by an NIH Bridge Grant from the Consortium for Functional Glycomics (GM62116, to R.D.C.) and NIH grant GM085448 (to D.F.S.). The authors have no financial interest to declare. We thank Jamie Heimburg-Molinaro for manuscript editing and review.

Received: July 14, 2008
Revised: October 23, 2008
Accepted: November 7, 2008
Published: January 29, 2009

REFERENCES

Babu, P., North, S.J., Jang-Lee, J., Chalabi, S., Mackerness, K., Stowell, S.R., Cummings, R.D., Rankin, S., Dell, A., and Haslam, S.M. (2008). Structural characterisation of neutrophil glycans by ultra sensitive mass spectrometric glycomics methodology. Glycoconj J. Published online June 28, 2008. 10.1007/s10719-008-9146-4.

Bigge, J.C., Patel, T.P., Bruce, J.A., Goulding, P.N., Charles, S.M., and Parekh, R.B. (1995). Nonselective and efficient fluorescent labeling of glycans using 2-amino benzamide and anthranilic acid. Anal. Biochem. *230*, 229–238.

Blixt, O., Head, S., Mondala, T., Scanlan, C., Huflejt, M.E., Alvarez, R., Bryan, M.C., Fazio, F., Calarese, D., Stevens, J., et al. (2004). Printed covalent glycan array for ligand profiling of diverse glycan binding proteins. Proc. Natl. Acad. Sci. USA *101*, 17033–17038.

Bohorov, O., Andersson-Sand, H., Hoffmann, J., and Blixt, O. (2006). Arraying glycomics: a novel bi-functional spacer for one-step microscale derivatization of free reducing glycans. Glycobiology *16*, 21C–27C.

Breuilh, L., Vanhoutte, F., Fontaine, J., van Stijn, C.M., Tillie-Leblond, I., Capron, M., Faveeuw, C., Jouault, T., van Die, I., Gosset, P., and Trottein, F. (2007). Galectin-3 modulates immune and inflammatory responses during helminthic infection: impact of galectin-3 deficiency on the functions of dendritic cells. Infect. Immun. *75*, 5148–5157.

Brewer, C.F. (2001). Lectin cross-linking interactions with multivalent carbohydrates. Adv. Exp. Med. Biol. *491*, 17–25.

Camby, I., Le Mercier, M., Lefranc, F., and Kiss, R. (2006). Galectin-1: a small protein with major functions. Glycobiology *16*, 137R–157R.

Cao, Z., Said, N., Amin, S., Wu, H.K., Bruce, A., Garate, M., Hsu, D.K., Kuwabara, I., Liu, F.T., and Panjwani, N. (2002). Galectins-3 and -7, but not galectin-1, play a role in re-epithelialization of wounds. J. Biol. Chem. *277*, 42299–42305.

Carlow, D.A., Williams, M.J., and Ziltener, H.J. (2003). Modulation of O-glycans and N-glycans on murine CD8 T cells fails to alter annexin V ligand induction by galectin 1. J. Immunol. *171*, 5100–5106.

Chandrasekaran, A., Srinivasan, A., Raman, R., Viswanathan, K., Raguram, S., Tumpey, T.M., Sasisekharan, V., and Sasisekharan, R. (2008). Glycan topology determines human adaptation of avian H5N1 virus hemagglutinin. Nat. Biotechnol. *26*, 107–113.

Chiu, M.H., Tamura, T., Wadhwa, M.S., and Rice, K.G. (1994). In vivo targeting function of N-linked oligosaccharides with terminating galactose and N-acetylgalactosamine residues. J. Biol. Chem. *269*, 16195–16202.

Cummings, R.D. (1994). Use of lectins in analysis of glycoconjugates. Methods Enzymol. *230*, 66–86.

de Boer, A.R., Hokke, C.H., Deelder, A.M., and Wuhrer, M. (2007). General microarray technique for immobilization and screening of natural glycans. Anal. Chem. *79*, 8107–8113.

Dumic, J., Dabelic, S., and Flogel, M. (2006). Galectin-3: an open-ended story. Biochim. Biophys. Acta *1760*, 616–635.

Elola, M.T., Wolfenstein-Todel, C., Troncoso, M.F., Vasta, G.R., and Rabinovich, G.A. (2007). Galectins: matricellular glycan-binding proteins linking cell adhesion, migration, and survival. Cell. Mol. Life Sci. *64*, 1679–1700.

Feizi, T., and Chai, W. (2004). Oligosaccharide microarrays to decipher the glyco code. Nat. Rev. Mol. Cell. Biol. *5*, 582–588.

Feizi, T., Fazio, F., Chai, W., and Wong, C.H. (2003). Carbohydrate microarrays—a new set of technologies at the frontiers of glycomics. Curr. Opin. Struct. Biol. *13*, 637–645.

Frigeri, L.G., Zuberi, R.I., and Liu, F.T. (1993). Epsilon BP, a beta-galactoside-binding animal lectin, recognizes IgE receptor (Fc epsilon RI) and activates mast cells. Biochemistry *32*, 7644–7649.

Guo, H.B., Nairn, A., Harris, K., Randolph, M., Alvarez-Manilla, G., Moremen, K., and Pierce, M. (2008). Loss of expression of N-acetylglucosaminyltransferase Va results in altered gene expression of glycosyltransferases and galectins. FEBS Lett. *582*, 527–535.

Hirabayashi, J., Hashidate, T., Arata, Y., Nishi, N., Nakamura, T., Hirashima, M., Urashima, T., Oka, T., Futai, M., Muller, W.E., et al. (2002). Oligosaccharide specificity of galectins: a search by frontal affinity chromatography. Biochim. Biophys. Acta *1572*, 232–254.

Karmakar, S., Stowell, S.R., Cummings, R.D., and McEver, R.P. (2008). Galectin-1 signaling in leukocytes requires expression of complex-type N-glycans. Glycobiology *18*, 770–778.

La, M., Cao, T.V., Cerchiaro, G., Chilton, K., Hirabayashi, J., Kasai, K., Oliani, S.M., Chernajovsky, Y., and Perretti, M. (2003). A novel biological activity for galectin-1: inhibition of leukocyte-endothelial cell interactions in experimental inflammation. Am. J. Pathol. *163*, 1505–1515.

Lagana, A., Goetz, J.G., Cheung, P., Raz, A., Dennis, J.W., and Nabi, I.R. (2006). Galectin binding to Mgat5-modified N-glycans regulates fibronectin matrix remodeling in tumor cells. Mol. Cell. Biol. *26*, 3181–3193.

Lajoie, P., Partridge, E.A., Guay, G., Goetz, J.G., Pawling, J., Lagana, A., Joshi, B., Dennis, J.W., and Nabi, I.R. (2007). Plasma membrane domain organization regulates EGFR signaling in tumor cells. J. Cell Biol. *179*, 341–356.

Lau, K.S., Partridge, E.A., Grigorian, A., Silvescu, C.I., Reinhold, V.N., Demetriou, M., and Dennis, J.W. (2007). Complex N-glycan number and degree of branching cooperate to regulate cell proliferation and differentiation. Cell *129*, 123–134.

Leffler, H., and Barondes, S.H. (1986). Specificity of binding of three soluble rat lung lectins to substituted and unsubstituted mammalian beta-galactosides. J. Biol. Chem. *261*, 10119–10126.

Leppanen, A., Stowell, S., Blixt, O., and Cummings, R.D. (2005). Dimeric galectin-1 binds with high affinity to alpha2,3-sialylated and non-sialylated terminal N-acetyllactosamine units on surface-bound extended glycans. J. Biol. Chem. *280*, 5549–5562.

Merkle, R.K., and Cummings, R.D. (1987). Lectin affinity chromatography of glycopeptides. Methods Enzymol. *138*, 232–259.

Nussler, A.K., Wittel, U.A., Nussler, N.C., and Beger, H.G. (1999). Leukocytes, the Janus cells in inflammatory disease. Langenbecks Arch. Surg. *384*, 222–232.

Ohtsubo, K., Takamatsu, S., Minowa, M.T., Yoshida, A., Takeuchi, M., and Marth, J.D. (2005). Dietary and genetic control of glucose transporter 2 glycosylation promotes insulin secretion in suppressing diabetes. Cell *123*, 1307–1321.

Opferman, J.T. (2008). Apoptosis in the development of the immune system. Cell Death Differ. *15*, 234–242.

Pueppke, S.G. (1979). Purification and characterization of a lectin from seeds of the winged bean, Psophocarpus tetragonolobus (L.)DC. Biochim. Biophys. Acta *581*, 63–70.

Rabinovich, G.A., Liu, F.T., Hirashima, M., and Anderson, A. (2007a). An emerging role for galectins in tuning the immune response: lessons from experimental models of inflammatory disease, autoimmunity and cancer. Scand. J. Immunol. *66*, 143–158.

Rabinovich, G.A., Toscano, M.A., Jackson, S.S., and Vasta, G.R. (2007b). Functions of cell surface galectin-glycoprotein lattices. Curr. Opin. Struct. Biol. *17*, 513–520.

Roseman, D.S., and Baenziger, J.U. (2001). The mannose/N-acetylgalactosamine-4-SO4 receptor displays greater specificity for multivalent than monovalent ligands. J. Biol. Chem. *276*, 17052–17057.

Rubinstein, N., Ilarregui, J.M., Toscano, M.A., and Rabinovich, G.A. (2004). The role of galectins in the initiation, amplification and resolution of the inflammatory response. Tissue Antigens *64*, 1–12.

Song, X., Xia, B., Lasanajak, Y., Smith, D.F., and Cummings, R.D. (2007). Quantifiable fluorescent glycan microarrays. Glycoconj. J. *25*, 15–25.

Stowell, S.R., Arthur, C.M., Mehta, P., Slanina, K.A., Blixt, O., Leffler, H., Smith, D.F., and Cummings, R.D. (2008a). Galectin-1, -2, and -3 exhibit differential recognition of sialylated glycans and blood group antigens. J. Biol. Chem. *283*, 10109–10123.

Stowell, S.R., Dias-Baruffi, M., Penttila, L., Renkonen, O., Nyame, A.K., and Cummings, R.D. (2004). Human galectin-1 recognition of poly-N-acetyllactosamine and chimeric polysaccharides. Glycobiology *14*, 157–167.

Stowell, S.R., Karmakar, S., Stowell, C.J., Dias-Baruffi, M., McEver, R.P., and Cummings, R.D. (2007). Human galectin-1, −2, and −4 induce surface exposure of phosphatidylserine in activated human neutrophils but not in activated T cells. Blood *109*, 219–227.

Stowell, S.R., Qian, Y., Karmakar, S., Koyama, N.S., Dias-Baruffi, M., Leffler, H., McEver, R.P., and Cummings, R.D. (2008b). Differential roles of galectin-1 and galectin-3 in regulating leukocyte viability and cytokine secretion. J. Immunol. *180*, 3091–3102.

Toscano, M.A., Bianco, G.A., Ilarregui, J.M., Croci, D.O., Correale, J., Hernandez, J.D., Zwirner, N.W., Poirier, F., Riley, E.M., Baum, L.G., and Rabinovich, G.A. (2007a). Differential glycosylation of TH1, TH2 and TH-17 effector cells selectively regulates susceptibility to cell death. Nat. Immunol. *8*, 825–834.

Toscano, M.A., Ilarregui, J.M., Bianco, G.A., Campagna, L., Croci, D.O., Salatino, M., and Rabinovich, G.A. (2007b). Dissecting the pathophysiologic role of endogenous lectins: glycan-binding proteins with cytokine-like activity? Cytokine Growth Factor Rev. *18*, 57–71.

Walzel, H., Fahmi, A.A., Eldesouky, M.A., Abou-Eladab, E.F., Waitz, G., Brock, J., and Tiedge, M. (2006). Effects of N-glycan processing inhibitors on signaling events and induction of apoptosis in galectin-1-stimulated Jurkat T lymphocytes. Glycobiology *16*, 1262–1271.

Wilker, P.R., Sedy, J.R., Grigura, V., Murphy, T.L., and Murphy, K.M. (2007). Evidence for carbohydrate recognition and homotypic and heterotypic binding by the TIM family. Int. Immunol. *19*, 763–773.

Xia, B., Kawar, Z.S., Ju, T., Alvarez, R.A., Sachdev, G.P., and Cummings, R.D. (2005). Versatile fluorescent derivatization of glycans for glycomic analysis. Nat. Methods *2*, 845–850.

Yamamoto, K., Tsuji, T., and Osawa, T. (1998). Analysis of asparagine-linked oligosaccharides by sequential lectin-affinity chromatography. Methods Mol. Biol. *76*, 35–51.